

## Supplemental Information

### Hydrogen reactivity on highly-hydroxylated TiO<sub>2</sub>(110) surface prepared via carboxylic acid adsorption and photolysis

Y. Du,<sup>a</sup> N. G. Petrik,<sup>\*b</sup> N. A. Deskins,<sup>\*c</sup> Z. Wang,<sup>a</sup> M. A. Henderson,<sup>b</sup> G. A. Kimmel,<sup>b</sup>  
and I. Lyubinetsky<sup>\*a</sup>

---

<sup>a</sup> Environmental Molecular Science Laboratory and Institute for Integrated Catalysis, Pacific Northwest National Laboratory, Richland, WA 99352, USA. E-mail: igor.lyubinetsky@pnl.gov;

<sup>b</sup> Fundamental & Computational Sciences Directorate and Institute for Integrated Catalysis, Pacific Northwest National Laboratory, Richland, WA 99352, USA. E-mail: .nikolai.petrik@pnnl.gov;

<sup>c</sup> Department of Chemical Engineering, Worcester Polytechnic Institute, Worcester, MA 01609, USA. E-mail: nadeskins@wpi.edu.

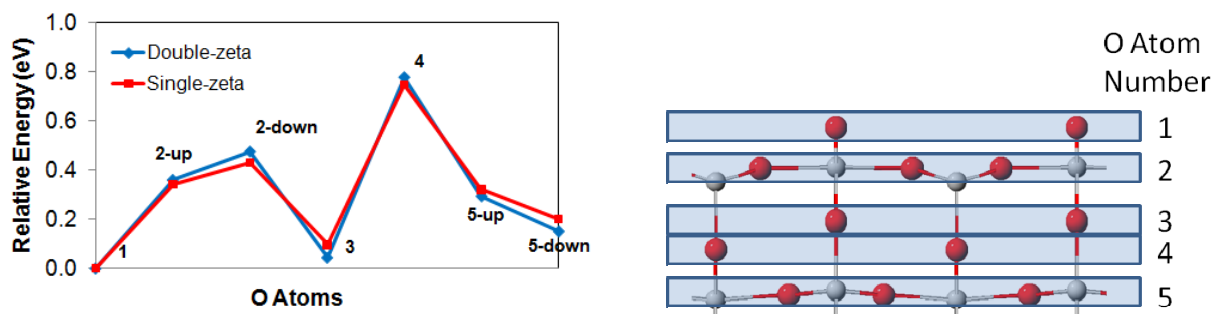


**Fig. S1.** Comparison of H diffusion energies into the bulk for double- $\zeta$  and single- $\zeta$  basis sets representing Ti. The surface initially had one  $\text{OH}_b$  that diffused into the bulk. The O atoms to which the H atom bonded are also shown. For example,  $\text{O}_1$  corresponds to the surface  $\text{O}_b$  atom.

Shown in Fig. S1 is a comparison of results using double- $\zeta$  and single- $\zeta$  basis sets for Ti. O and H both have double- $\zeta$  basis sets. These test calculations were performed with a surface having one  $\text{OH}_b$  that diffused into the bulk. The results show that using a single- $\zeta$  basis sets for Ti had negligible effect on the H diffusion energies. Similar results were obtained for a surface having two  $\text{OH}_b$ . We therefore used single- $\zeta$  Ti basis sets in our work.

**S2:** STM movie (S2.avi) showing the highly-hydroxylated  $\text{TiO}_2(110)$  surface at 300 K, illustrating along- and across-row diffusion of H species (as marked by ovals and rectangulars, respectively). (Acquisition time was  $\sim 126$  s per frame).

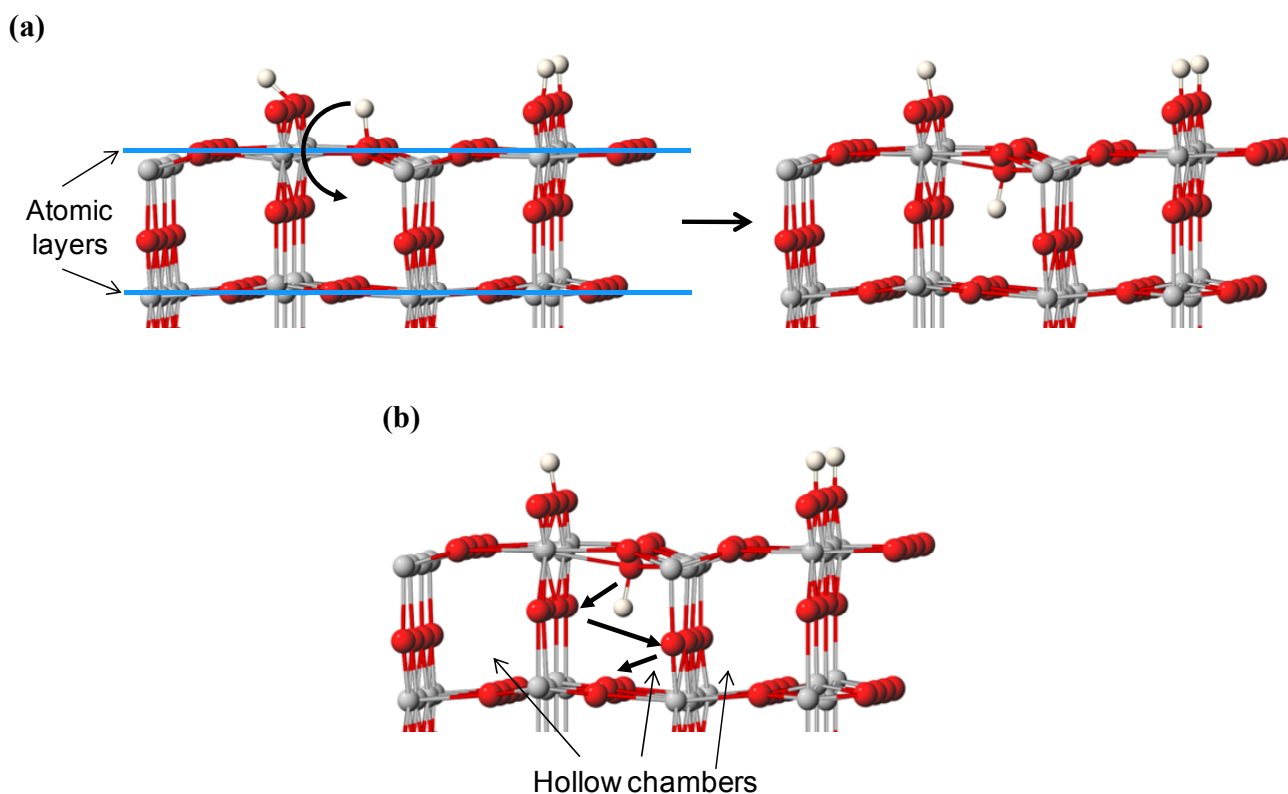


**Fig. S3.** Illustration of the H diffusion processes. (a) H transfer across atomic layers and (b) H transfer within a hollow chamber.

The two general processes for H diffusion are shown in Fig. S3. The first process involves H transfer across an atomic layer (Fig. S3(a)), which is essentially an OH rotation of the H attached to the same O atom. This process occurs with an activation barrier of  $\sim 1$  eV. The barrier for crossing the first atomic layer is 1.04 eV (shown in the main text as 'B' to 'C') and for crossing the second atomic layer is 1.05 eV (not shown in the main text). The second process involves H transfer from one O atom to a neighboring O atom. These O atoms are all within a 'hollow chamber' (indicated in Figure S2(b)) and do not involve crossing any atomic layers. Barriers for these H transfers are near 0.5 eV ('C' to 'D' and 'D' to 'E' in the main text).

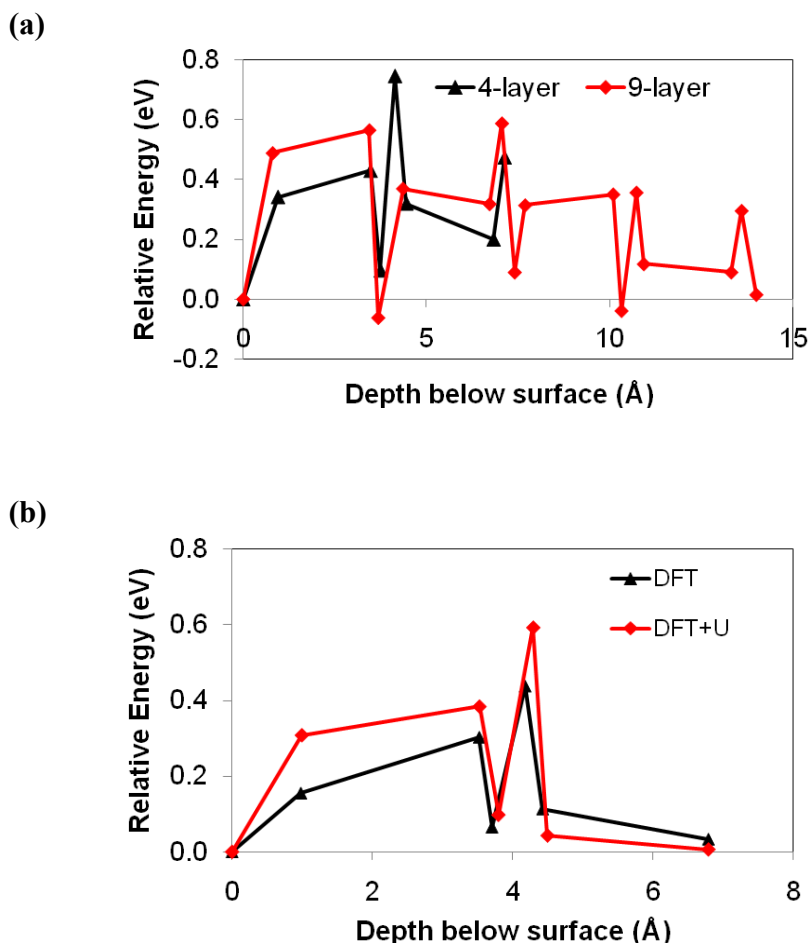


**Fig. S4.** (a) Effect of number of O-Ti-O tri-layers on H diffusion into the bulk. Each point represents a stable site for an OH. Results for slabs with four and nine layers are given. (b) Effect of employing DFT+U on H diffusion into the bulk. A four-layer slab with a U value of 4.1 eV was used for these calculations.

We tested the effect of using a larger slab in modeling bulk diffusion. Figure S4(a) shows the stable energies for OH groups in a 4- and 9-layer slab (each layer represents 3 atomic layers or an O-Ti-O tri-layer). The surface OH<sub>b</sub> group is taken as the 'zero' energy. The energy trends for the two slabs are very similar and have the same basic shape. In the 9-layer slab the energies for OH species are sometimes higher in energy than the OH species in the 4-layer slab, while occasionally some are lower in energy. There are even a few OH species in the 9-layer slab that are slightly exothermic or close to zero in energy. The majority of OH species however are endothermic, indicating that there is no large thermodynamic driving force for H diffusion into the bulk. We did not calculate activation energies for the 9-layer slab, but expect them to be similar to those calculated using the 4-layer slab. We also used the DFT+U method (U = 4.1 eV applied to Ti d electrons) and found similar OH energies for the DFT and DFT+U methods as shown in Figure S4(b), indicating that inclusion of the U correction does not change our conclusions.

**S5:** We define the branching ratio as the ratio of the rate of H<sub>2</sub>O desorption to rate of H diffusion ( $k_{\text{H}_2\text{O-desorp}}/k_{\text{H-diff}}$ ). Using transition state theory we can arrive at the following definition of the branching ratio:

$$\text{branching ratio} = \frac{\nu_{\text{H}_2\text{O-desorption}} \cdot e^{-\Delta G_{\text{H}_2\text{O-desorption}}^\ddagger / k_B T}}{\nu_{\text{H-diffusion}} \cdot e^{-\Delta G_{\text{H-diffusion}}^\ddagger / k_B T}},$$

where  $\nu$  and  $\Delta G^\ddagger$  are pre-exponential frequencies and activation free energies, respectively. Accordingly, the activation free energy is defined as  $\Delta G^\ddagger = \Delta E^\ddagger + \Delta pV^\ddagger - T\Delta S^\ddagger$ . Again, assuming pressure-volume and entropic changes are negligible in the solid phase ( $\Delta G_{\text{solid}}^\ddagger \approx \Delta E_{\text{solid}}^\ddagger$ ) we take  $\Delta G_{\text{H-diffusion}}^\ddagger$  to be the largest calculated barrier, which corresponds to 1.04 eV ('B' to 'C' in Figure 7). On the other hand, since H<sub>2</sub>O desorption involves a change of state (solid to gas phase), we cannot assume  $\Delta S^\ddagger$  and  $\Delta pV^\ddagger$  to be negligible. As Figure 6 shows, the transition state lies very close to the final state (the process is an 'uphill' climb) and therefore the  $\Delta S^\ddagger$  and  $\Delta pV^\ddagger$  values will be very similar to the same values of the final state (H<sub>2</sub>O desorbed off the surface). We can therefore approximate the  $\Delta G_{\text{H}_2\text{O-desorption}}^\ddagger$  to be  $\Delta E_{\text{H}_2\text{O-desorption}}^\ddagger + TS_{\text{H}_2\text{O}} - pV_{\text{H}_2\text{O}}$ , similar to Equation 9. As discussed in our methodology section (Section 2),  $S_{\text{H}_2\text{O}}$  and  $pV_{\text{H}_2\text{O}}$  values were taken from experimental data.<sup>51</sup> Finally, we presumed the pre-exponential frequencies of the two processes to be equivalent, based on the assumption that the frequencies are of similar magnitudes ( $\sim 10^{13} \text{ s}^{-1}$ ). Such an approximation may not be fully correct, but the branching ratio will largely be dominated by the ratio of exponentials, and our conclusions will not change when more rigorous methods are applied to determining the pre-exponential frequencies.